disturbance decays more slowly than $x^{-1/2}$. This is a consequence of the ever increasing displacement thickness. Since the boundary layer does not allow the flow to expand to its original state, the expansion from the viscous layer is slower than a centered expansion and cannot decrease the shock strength as rapidly.

Results

These results may now be applied to that disturbance generated by a viscous boundary layer. The displacement thickness in a compressible fluid is a function of several parameters. Since we only wish to illustrate the theory, the displacement thickness for an incompressible flow is used.

For an external flow with a Reynolds number of 10^5/cm, the displacement thickness corresponding to an incompressible laminar boundary layer is

$$\delta^* = 6 \times 10^{-3} x^{1/2} \qquad (x - cm)$$

Similarly, the displacement thickness for a turbulent boundary layer is:

$$\delta^* = 4 \times 10^{-3} (x)^{0.86}$$

The density perturbations behind a shock attenuated by laminar and turbulent boundary layers in a Mach 4 flow are illustrated in Fig. 2. A schematic diagram of the shock waves is also presented. The laminar results are applicable beyond the boundary-layer transition length because the waves from the boundary layer require a finite time to reach the shock. The origin of the waves striking the shock at x_s is indicated in Fig. 3.† Transition to turbulence at a Reynolds number of 10^5 would correspond to $x_w = 1$ cm. Figure 3 indicates that this would be felt by the shock about 2 m downstream. Thus, the laminar results in Fig. 2 are appropriate for $x_s < 2$ m. Laminar results are valid beyond $x_s = 2$ m when transition occurs at higher Reynolds numbers.

The analysis of the shock that is driven by the turbulent boundary layer does not include the effect of the initial "laminar" shock. Thus, it is valid only as $x_s \to \infty$ and it is not an accurate description of the flow just downstream of the point where the two shocks coalesce.

Conclusions

Whitham's "area rule" has been applied to disturbances generated by power law bodies in an otherwise uniform two-dimensional flow. It has been shown that the shocks produced by such bodies decay more slowly than those from bodies of finite extent.

The results have been applied to disturbances generated by a viscous boundary layer. For the case cited previously, the application of acoustics is valid for $x_s > 1$ cm ($\Delta\rho/\rho|_s < 0.1$) and density disturbances of the order of a few percent are shown to exist for several meters.

References

[1] Gerry, E. T., "The Gas Dynamic Laser," *Laser Focus*, Dec. 1970, p. 27.

[2] Sedov, L. I., *Similarity and Dimensional Methods in Mechanics*, Academic Press, New York, 1959.

[3] Hayes, W. D. and Probstein, R. F., *Hypersonic Flow Theory*, Academic Press, New York, 1959.

[4] Lighthill, M. J., "A Technique for Rendering Approximate Solutions to Physical Problems Uniformly Valid," *Philosophical Magazine*, Vol. 40, 1949, pp. 1179–1201.

[5] Friedrichs, K. O., "Formation and Decay of Shock-Waves," *Communications on Pure and Applied Mathematics*, Vol. 1, No. 3, 1948, p. 211.

[6] Lighthill, M. J., "Higher Approximations in Aerodynamic Theory," *General Theory of High Speed Aerodynamics*, edited by W. R. Sears, Princeton University Press, Princeton, N. J., 1954, p. 444.

[7] Whitham, G. B., "The Flow Pattern of a Supersonic Projectile," *Communications on Pure and Applied Mathematics*, Vol. 5, 1952, pp. 301–349.

[8] Simons, G. A., "The Propagation of Aerodynamic Disturbances in Gas Dynamic Lasers," RR 356, Nov. 1970, Avco Everett Research Laboratory, Everett, Mass.

† Since $\Delta\rho/\rho$ is constant on a wave, $x_w(x_s)$ is determined from Eqs. (2) and (4).

Slipstream Formed by a Supersonic Source in a Hypersonic Stream

ANTHONY M. AGNONE*
New York University, New York

MANY fluid flow phenomena exhibit somewhat similar flowfield features. For example, the flow pattern produced by a high-pressure jet issuing into an oncoming stream is somewhat similar to that of a retrofiring rocket nozzle descending into a thin atmosphere at hypersonic speeds, or to a high intensity explosion moving at great speeds in a fluid ambient. Besides its inherent academic interest, some general features of the aforementioned flows can be assessed by considering a simplified flow model which approximates these flows in a certain limit.

To this end we consider the flowfield produced by a supersonic source of radius r^* which spews out fluid into an oncoming hypersonic stream as shown in the lower half of Fig. 1. In the hypersonic limit ($M_\infty \to \infty$, $\gamma \to 1$) and when the source strength becomes large, so that the ratio of the centerline distance of the shock system from the center of the source to the source radius is large ($r_0/r^* \gg 1$), the shock surfaces and contact surface can be considered as a single surface. This contact surface separates a uniform freestream from an equally isentropic source flow. It is the purpose of this Note to determine the shape of this limiting surface.

The shape of the slipstream is uniquely determined from the requirement that the pressure be equal on both sides of the slip-surface and from geometric constraints. The geometric constraint arise from the fact that the slip-surface must lie between the vertical and the normal to the radial vector as shown in the upper half of Fig. 1.

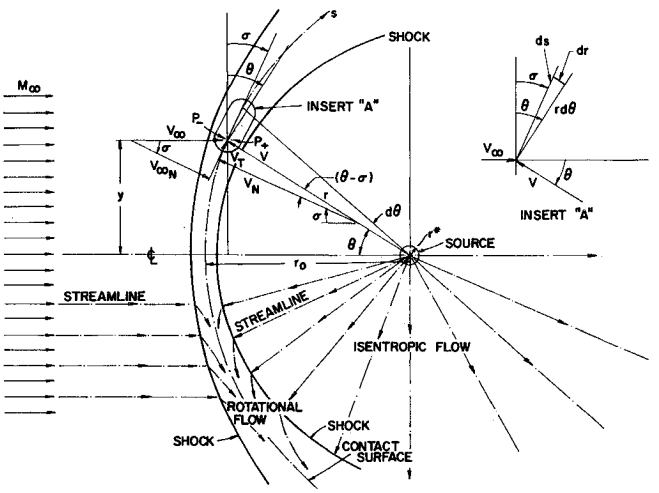

Fig. 1 General features of the flowfield produced by a supersonic source in a hypersonic stream.

Received January 6, 1971; revision received February 17, 1971. This work was supported by NASA under NASA Grant NGR 33-016-131.

* Assistant Research Scientist. Associate Member AIAA.

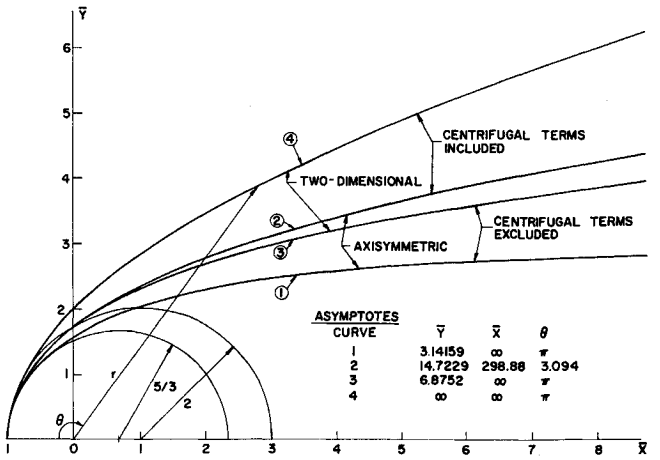

Fig. 2 Slipstream shapes.

The pressure on the freestream side of the contact surface is given by a Newtonian pressure distribution corrected for Busemann centrifugal pressure

$$p_- = p_\infty \left\{1 + \gamma_\infty M_\infty^2 \cos^2\sigma - \frac{\gamma_\infty M_\infty^2}{y^j}\left(\int_0^{y_1} y^j \sin\sigma dy\right)\frac{d\sin\sigma}{dy}\right\} \quad (1)$$

A derivation of this equation is given in Ref. 1.

The pressure on the source side of the contact surface can be found in an anologous fashion and can be shown to be equal to

$$p_+ = p \left\{1 + \gamma M^2 \cos^2(\theta - \sigma) + \frac{1}{y^j}\left(\int_0^{y_1} \gamma M^2 y^j \frac{\sin 2(\theta - \sigma)}{2\cos\sigma} dy\right)\frac{d\sin\sigma}{dy}\right\} \quad (2)$$

in which the integral is taken to the edge of the inner shock layer. In this equation the first term is the stream static pressure; the second term is the component of the stream dynamic pressure normal to the slipstream; and the third term represents the centrifugal pressure which is proportional to the product of the tangential momentum of the fluid in the shock layer and the curvature of the slipstream. The variables ρ, V, p, M are functions of r according to the source solution. The symbol $j = 0$ represents a two-dimensional (cylinder) source and $j = 1$ represents a spherical source.

The flowfield properties of the source are functions of the radial distance from the center of the source through the one-dimensional flow equations.[2] For example, the local Mach number at large distances from the center of the source is given by

$$M \approx [(\gamma + 1)/(\gamma - 1)]^{(\gamma+1)/4}(r/r^*)^{(j+1)(\gamma-1)/2} \quad (3)$$

The equations required for uniquely determining the slipstream shapes are

$$p_-(\sigma, y; \gamma_\infty, M_\infty) = p_+(\sigma, \theta, y; \gamma, M) \quad (4)$$

where

$$y = r\sin\theta \quad (5a)$$

and from geometry

$$dr/d\theta = r\tan(\theta - \sigma) \quad (5b)$$

Here σ and r are the two unknown functions of θ.

At the centerline ($\theta = 0$, $\sigma = 0$) Eq. (4) gives

$$p_\infty(1 + \gamma_\infty M_\infty^2) = p_0(1 + \gamma M_0^2) \quad (6)$$

where the subscript 0 denotes centerline conditions. In terms of the jet and freestream stagnation pressures and for large M_0 and M_∞ this relation simplifies to

$$M_0 \approx M_\infty(p_{tj}/p_{t\infty})^{(\gamma-1)/2} \quad \text{when} \quad \gamma_\infty = \gamma_j = \gamma \quad (7)$$

The centerline distance to the shock is

$$\left(\frac{r_0}{r^*}\right)^{j+1} \approx \left(\frac{p_{tj}}{p_{t\infty}}\right) M_\infty^{2/(\gamma-1)} \left(\frac{\gamma - 1}{\gamma + 1}\right)^{[\gamma+1]/2(\gamma-1)} \quad (8)$$

To assess the extent of the influence of the centrifugal pressure terms on this shape a solution of the above equations is obtained first by neglecting these terms and then by including them.

Neglecting both free stream static pressure and the centrifugal pressure terms, Eq. (4) reduces to

$$\cos(\theta - \sigma) = f(r)\cos\sigma \quad (9)$$

where

$$f(r) = \left(\frac{p_\infty}{p}\right)^{1/2}\frac{M_\infty}{M} \quad (10)$$

After substituting for $p(r)$ and $M(r)$ from the source solution, taking the limit for large M_∞ and M_0 and nondimensionalizing r with respect to r_0 we find

$$f(\bar{r}) \cong \bar{r}^{(j+1)/2} \quad (11)$$

Elimination of σ from Eq. (5b)

$$\tan\sigma = f(\bar{r})\csc\theta - \cot\theta \quad (12)$$

and

$$d\bar{r}/d\theta = [\bar{r}/f(\bar{r})]\csc\theta - \bar{r}\cot\theta \quad (13)$$

This equation is subject to the initial condition at $\theta = 0\ \bar{r} = 1$.

For the spherical source $f(\bar{r}) = \bar{r}$ (11a). The equation is a Bernoulli type equation and its solution is

$$\bar{r} = \theta/\sin\theta \quad (14a)$$

or

$$y = \theta \quad (14b)$$

It is interesting to note that this solution is identical to the incompressible case.[3] The slope of the slipstream is then given by

$$\tan\sigma = \theta\csc^2\theta - \cot\theta \quad (15)$$

For the cylindrical source

$$f(\bar{r}) = (\bar{r})^{1/2} \quad (15a)$$

the differential equation is again of Bernoulli type if we let

$$t = (\bar{r})^{1/2} \quad (16)$$

The resulting solution is

$$\bar{r} = 2F^2(\varphi, 45°)/\sin\theta \quad (17a)$$

or

$$\bar{y} = 2F^2(\varphi, 45°) \quad (17b)$$

Where

$$F(\varphi, k) = \int_0^\varphi (1 - k^2\sin^2\varphi)^{-1/2} d\varphi \quad (18a)$$

and

$$\varphi = \sin^{-1}\{2\sin(\theta/2)/[1 + \sin(\theta/2) + \cos(\theta/2)]\}^{1/2} \quad (18b)$$

The slope is given by

$$\tan\sigma = 2^{1/2}F(\varphi, 45°)/\sin^{3/2}\theta - \cot\theta \quad (19)$$

To determine the change in the slipstream shape due to the centrifugal terms, the pressure relation is rewritten, neglecting the static pressure terms which are important only in the tail region, as follows

$$d\sigma/d\theta = \sin^j\theta[R\cos^2\sigma - \cos^2(\theta - \sigma)]/g(\theta)\cos(\theta - \sigma) \quad (20a)$$

where

$$dg/d\theta = \sin^j\theta[R\sin 2\sigma + \sin 2(\theta - \sigma)]/2\cos(\theta - \sigma) \quad (20b)$$

and

$$R = r^{j+1} \quad (20c)$$

$$dy = [r\cos\sigma/\cos(\theta - \sigma)]d\theta \quad (20d)$$

has been substituted. Here $g(\theta)$ represents the growth of the tangential momentum in the shock layers. The preceding equation shows that the slipstream curvature is proportional to the ratio of the difference in the normal component of the dynamic pressure to the tangential momentum.

The geometric condition

$$dR/d\theta = (j + 1)R\tan(\theta - \sigma) \quad (20e)$$

together with the initial conditions at

$$\theta = 0, \quad \sigma = 0, \quad R = 1, \quad g = 0 \quad (20f)$$

form a system of three nonlinear ordinary differential equations for the three unknowns σ, R, g.

For the two-dimensional source $j = 0$, the aforementioned system admits a simple solution

$$\sigma = \theta/2 \quad (21)$$

This implies the curvature factor $d\sigma/d\theta$ is a constant. The geometric condition gives

$$\bar{r} = 1/\cos^2(\theta/2) \quad (22)$$

and integration of the tangential momentum growth equation yields

$$g(\theta) = 2\tan(\theta/2)\sin(\theta/2) \quad (23)$$

For the spherical source a series solution is obtained for $\theta \ll 1$ by noting that due to symmetry

$$R = 1 + R_0''\theta^2/2! + R_0''''\theta^4/4! + \ldots \quad (24)$$

and

$$\sigma = \sigma_0'\theta + \sigma_0'''\theta^3/3! + \ldots \quad (25)$$

in which the primes denote differentiation with respect to theta. Here σ_0' is recognized to be the curvature of the slipstream at the centerline. Substituting these expansions into the differential equation for g and integrating gives

$$g(\theta) = \theta^{j+2}/(j + 2) - (\sigma_0'R_0'' - \tfrac{1}{3}\sigma_0'^3 - \tfrac{4}{3} + 3\sigma_0' - 3\sigma_0'^2)\theta^{j+3}/2(j + 3) + \tfrac{1}{2}(1 - 2\sigma_0' + \sigma_0'^2 - j/3)\theta^{j+4}/(j + 4) + \ldots \quad (26)$$

The differential equation for the curvature evaluated at $\theta = 0$ gives

$$\sigma_0' = (j + 2)(R_0'' + 2)/2(2j + 5) \quad (27)$$

The geometric condition differentiated once and evaluated at $\theta = 0$ gives

$$R_0'' = (j + 1)(1 - \sigma_0') \quad (28)$$

From which

$$\sigma_0' = (j + 2)/(j + 4) \quad (29)$$

and

$$R_0'' = 2(j + 1)/(j + 4) \quad (30)$$

The series solution for $\bar{r}$ and σ become

$$\bar{r} = 1 + [1/(j + 4)]\theta^2 + \ldots \quad (31)$$

$$\sigma = (j + 2)/(j + 4)\theta + \ldots \quad (32)$$

A numerical integration of this system was obtained with the help of a CDC 6600 computer. Numerical accuracy of 0.01% was imposed at each integration step by using Runge-Kutta integration with variable step size. The results of this computation are shown graphically on Fig. 2 along with the analytic solution and the series expansion.

The slipstream shapes differ significantly for theta greater than approximately one radian by the inclusion or deletion of the centrifugal terms. This departure is largely due to increasing tangential momentum in the shock layers and not so much to the curvature of the slipstream.

References

[1] Hayes, W. D. and Probstein, R. F., *Hypersonic Flow Theory*, Academic Press, New York, 1959, p. 78.

[2] Milne-Thomson, L. M., *Theoretical Hydrodynamics*, Macmillan, New York, 1955.

[3] Prandtl, L. and Tietjens, O. G., *Fundamentals of Hydro- and Aeromechanics*, Dover, New York, 1957, p. 147.

Experimental Investigation of the Lee-Side Flow from a Cone-Cylinder Model

Alfred M. Morrison* and Charles W. Ingram†
University of Notre Dame, Notre Dame, Ind.

Introduction

One phase of the general problem of the interference between component parts of flight vehicles is the interference effects resulting from vortex shedding from a body of revolution at high angles of attack. When the angle of attack is small the boundary layer beings to thicken rapidly on the lee side of the body near the base. As the angle of attack or length fineness ratio is increased this phenomena progresses until the boundary layer separates from the body and two regions of concentrated vorticity are formed on the lee side. At this point the influences of inertia and viscosity of the air flowing around the body can no longer be neglected. The formation of the vortices results in a pressure reduction which increases the cross forces substantially more than potential flow theory would lead one to believe. Wind-tunnel tests have shown that these vortices have a large effect upon the forces developed on wing and tail surfaces.[1] Certain methods exist for estimating the forces developed on the wing and tail surfaces provided the positions and strengths of the body vortices are known.[1-4] The purpose of this Note is to present an experimental method for determining the position of the vortex core regions from subsonic wind-tunnel tests.

Experimental Procedure

The smoke flow visualization techniques of Brown[5] were used in this investigation. In order to obtain proper visualization of the flow, a converging slit-camera technique was employed. A schematic representation of this process is presented in Fig. 1. The technique employed two wind-

Received January 11, 1971; revision received February 16, 1971.

* Graduate Student, Research Assistant. Associate Member AIAA.

† Assistant Professor of Aerospace and Mechanical Engineering. Member AIAA.